GA-USTAR Phase 1: Development and Flight Testing of the Baseline Upset and Stall Research Aircraft

Or D. Dantsker,[*] Gavin K. Ananda,[†] and Michael S. Selig[‡]

Department of Aerospace Engineering, University of Illinois at Urbana–Champaign, Urbana, IL 61801, USA

The General Aviation Upset and Stall Testing Aircraft Research (GA-USTAR) project described in this paper aims to develop a dynamically-scaled, Reynolds number corrected, GA aircraft to provide validation data sets for the stall/upset aerodynamic model development. This paper describes the first of three phases of the GA-USTAR project, where the baseline aircraft was developed such that future modifications could be performed to dynamically-scale and then perform Reynolds number corrections to the aircraft. From the possible GA aircraft radio control models available, a 1/5-scale model Cessna 182 was chosen. The aircraft was first built as a radio control model with modifications being made to support future activities. The aircraft was instrumented with a high-fidelity data acquisition system, which was then used to collect baseline flight characteristics of the aircraft. Extensive flight testing was carried out with flight maneuvers performed according flight simulator qualification standards. A sampling of these maneuvers together with all aircraft state details is presented. These maneuvers included idle decent (gliding), elevator-induced phugoid dynamics, roll rate response, rudder response, stall (clean) with low rate elevator deflections, stall (clean) with high rate elevator deflections, and finally stall (half flaps) with high rate elevator deflections. The results presented show high quality aircraft state data that in the future will be used for validation of flight simulation aerodynamic models.

Nomenclature

CAD	=	computer-aided-design
CG	=	center of gravity
DOF	=	degree of freedom
GA	=	general aviation
ESC	=	electronic speed controller
GPS	=	global positioning system
IMU	=	inertial measurement unit
PWM	=	pulse width modulation
RC	=	radio control
a_x, a_y, a_z	=	body-axis translational acceleration
P	=	static pressure
p, q, r	=	roll, pitch and yaw rates
T	=	ambient temperature
u, v, w	=	body-fixed translational velocity
V_N, V_E, V_D	=	inertial-fixed translational velocity in NED coordinate system
V	=	speed
x, y, z	=	inertial-fixed position in ENU coordinate system
α	=	angle of attack
β	=	sideslip angle
δ	=	control surface deflection
ϕ, θ, ψ	=	roll, pitch and heading angles

---

[*]Graduate Research Fellow, AIAA Student Member. dantske1@illinois.edu
[†]Graduate Student (Ph.D. Candidate), AIAA Student Member. anandak1@illinois.edu
[‡]Professor, AIAA Associate Fellow. m-selig@illinois.edu

American Institute of Aeronautics and Astronautics

I. Introduction

The General Aviation Upset and Stall Testing Aircraft Research (GA-USTAR) project aims to develop a dynamically-scaled, Reynolds number corrected, General Aviation (GA) aircraft to provide validation data sets for the stall/upset aerodynamic model development.[1] Although dynamically-scaled models have been widely used in GA research (NASA Stall/Spin Research Program[2,3]), there has not been recent substantial work in stall/upset modeling and research for GA aircraft and therefore the GA-USTAR project intends to fill that void. This is a critical issue that needs to be addressed as according to the National Transportation and Safety Board (NTSB) Review of Civil Aviation Accidents from 2010[4] and the NTSB 2015/2016/2017 Most Wanted Transportation Safety Improvements factsheets,[5–7] fixed-wing general aviation (GA) accidents accounted for 89% of all accidents and 86% of total fatalities of U.S. civil aviation, where loss of control accounted for approximately 48% of these fatal accidents. The NASA Airborne Subscale Transport Aircraft Research (AirSTAR) Program[8–11] used dynamically-scaled vehicles to improve of commercial transport stall models. However, this has not been expanded to GA stall and upset.

The GA-USTAR project therefore focuses on the development and flight testing of a sub-scale GA aircraft for stall/upset aerodynamic modeling. To design and build a correct model, research was conducted to determine the requirements, such as dynamically scaling the aircraft, not only in terms of mass but also in terms of moments of inertia, Additional effort was put into researching a methodology to modify the aircraft flight surfaces to properly take into account Reynolds number effects. The design methodology as well as the flight testing protocols for the GA-USTAR project are outlined by Ananda, et al.[1] This paper will encompass the first of the three project phases, where the baseline aircraft that future revisions will be based on is developed. The second and third phase will take into account dynamic scaling and then Reynolds number corrections, respectively.

From a list of potential GA aircraft radio control models available, a 1/5-scale model Cessna 182 made by Top Flite[12] was chosen as the GA-USTAR aircraft.[1] The aircraft was first built as a radio control model, with some modifications being made to support Phases 2 and 3 of the project, and then was flight tested to ensure its airworthiness. The aircraft was then instrumented with an Al Volo FDAQ[13] data acquisition system, a XSens MTi-G-700[14] inertial measurement unit (IMU) and global position system (GPS), and a pitot-static probe. The instrumented aircraft was then flight tested through a variety of maneuvers that were designed to validate aerodynamic models for use in flight simulation. In this paper, the COTS R/C Cessna 182 aircraft will be referred as either the Phase 1 GA-USTAR aircraft or the baseline aircraft.

Flight tests for the GA-USTAR project were designed specifically based on 14 CFR Part 60 requirements[15] regarding extended envelope qualification performance standards for flight simulation training devices. Obviously, the full qualification standards are beyond the scope of this project. However, what is within the scope of this project is necessary flight tests outlined in the 14 CFR Part 60 document for the primary purpose of validating the aerodynamic models in flight simulators which include the basic aerodynamic performance of the aircraft modeled to the key characterization of the aerodynamics of an aircraft in stall/post-stall.

In this paper, a sampling of flight test data taken with the baseline GA- USTAR aircraft is presented. These flight tests include idle decent (gliding), elevator-induced phugoid, aileron roll rate response, rudder response, stall with low rate elevator and without flaps, stall with high rate elevator and without flaps and finally stall with high rate elevator and half flaps. These maneuvers will each be used toward validating aerodynamic models developed and a first step towards making a high-fidelity stall/upset aerodynamic model.[16]

This paper will provide details about the development of the baseline GA-USTAR aircraft, including the airframe construction, modeling, and instrumentation. Specifications for the aircraft and the instrumentation system will be given. This will be followed by a description of the data reduction. After that, the results of the flight testing will be presented. Finally conclusions and future work will be discussed.

American Institute of Aeronautics and Astronautics

II. Baseline GA-USTAR Development

The development of the baseline GA-USTAR aircraft was split into two stages: airframe construction and instrumentation. The completed aircraft and instrumentation specifications are presented in Section II.C.

A. Airframe Construction

The baseline GA-USTAR was developed based upon the experience gained developing and operating both the UIUC Aerotestbed, used for spin and upset testing,[17,18] and the UIUC Subscale Sukhoi, used for high angle-of-attack flight testing.[19] As with the past aircraft, the intended mission determined how it would be built. As the Top Flite Cessna 182 airframe (shown in Fig. 1) would be used to record flight data and eventually be loaded up with weight for dynamic scaling, the aircraft had to be extensively modified from the manufacturer instructions.

Modifications to the Cessna airframe started with changing the linkage configuration for the elevators from one servo controlling both elevator halves through a coupler located at the hinges, to two independent servos being used. Figure 2(a) shows the elevator and rudder linkages in the tail. The change added redundancy in the pitch control of the aircraft as well as allows for fine tuning of each elevator deflection angles; however, this requires the addition of a second servo. The original side elevator and rudder servo trays were replaced with a full, side-to-side tray in the center of the fuselage, which was cut to support the additional elevator servo, and can be seen in Figure 2(b). The tray was also used to mount a Smart-Fly power distribution system,[20] which was installed to increase control power redundancy as it features a dual power regulator. The power distribution system also helps to to decrease the wiring complexity in the aircraft as the unit duplicates servos signals passing through it from the receiver to the servos, allowing the data acquisition system to read these signals without requiring additional wiring harnesses.

The next set of notable modifications to the airframe was the mounting of the electric motor propulsion system elements. As with previous aircraft, using an electric motor was deemed favorable because of the near constant performance, increased reliability, and low vibrations; the increase in aircraft weight caused by using an electric motor compared to an internal combustion engine was actually desirable for the dynamically scaling of the aircraft.[1] The manufacturer did provide the option to use an electric power system; however, the wooden mount that supports the motor and electronic speed controller (ESC) was rather cumbersome. Additionally, the standard underside access battery mounting location limited battery size, which was very undesirable. Instead the motor was mounted using simple aluminum standoffs, which were fastened directly to the firewall, and the ESC was mounted to the bottom standoffs using plastic mounting tabs, as can be seen in Figure 2(c). The battery was moved from the under-access location and onto the fuel tank tray inside the aircraft. The tray provides enough room to mount a variety of different motor batteries; however, it does require the aircraft operator to remove the wings in order to swap the motor batteries. The fuel tank tray also was set up to support the two power distribution system batteries. As with past testbeds, a electric motor system safety power switch was also added to increase operator safety. The rest of the airframe build followed the manufacturer instructions.

Figure 1. The baseline GA-USTAR aircraft (1/5-Scale Top-Flite Cessna 182).

American Institute of Aeronautics and Astronautics
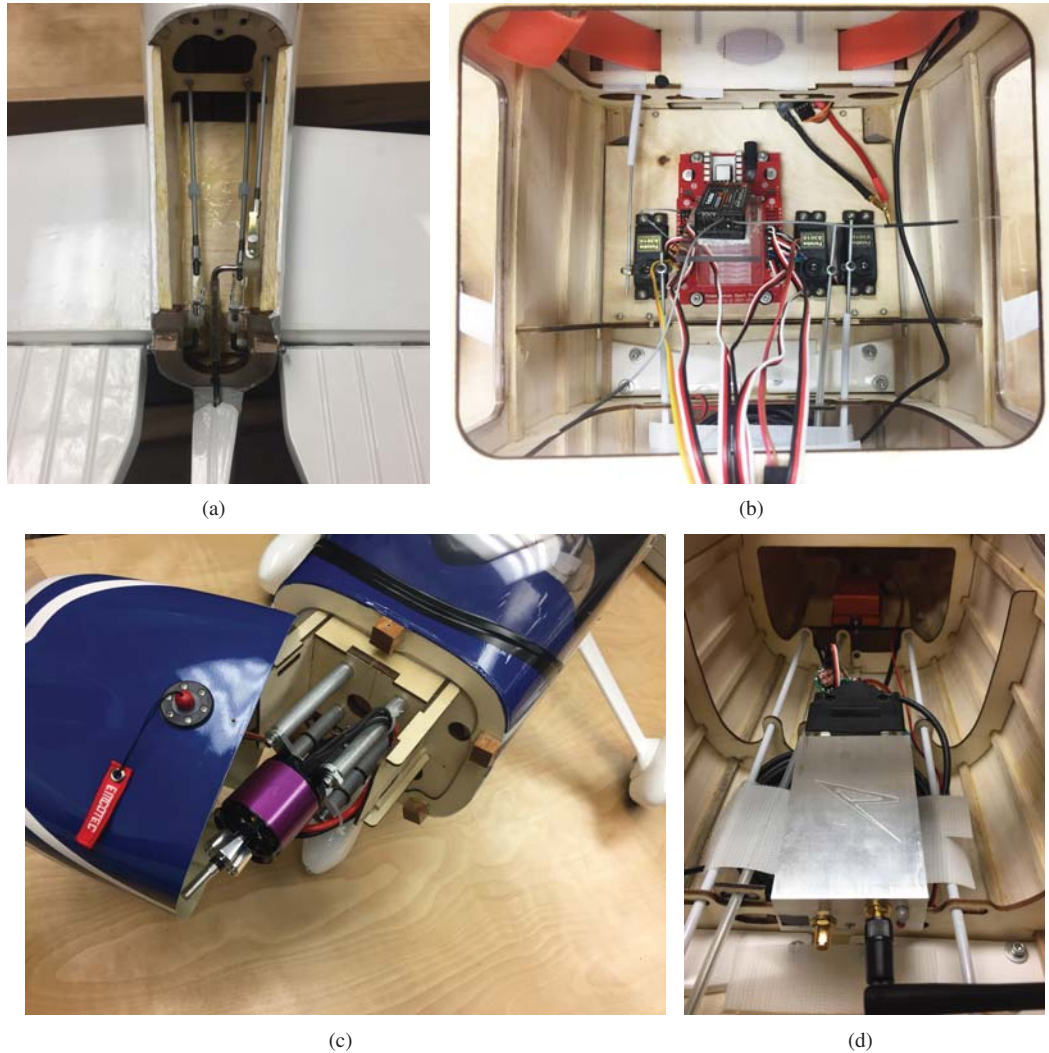
(a)

(b)

(c)

(d)

Figure 2. Construction details in baseline GA-USTAR aircraft: (a) tail dual elevator and rudder linkage arrangement, (b) custom front tray holding the two elevator servos, rudder servo, Smart-Fly power distribution system, and the receiver, (c) nose with the motor, ESC, and safety power switch visible, and (d) Al Volo FDAQ flight data acquisition system and the XSens MTi-G-700 IMU mounted in the aircraft rear.

B. Instrumentation

The aircraft was instrumented with a high-fidelity Al Volo FDAQ[13] data acquisition system. The system operates at 400 Hz and integrates with a 9 degree-of-freedom (9-DOF) XSens MTi-G-700[14] IMU with a GPS receiver among many other sensors. The Al Volo FDAQ and the XSens MTi-G-700 can be seen installed in the rear of the aircraft fuselage in Figure 2(d). A pitot-static probe was installed half-way down the span of the left wing and connects to a differential pressure transducer, which is wired into an analog input on the FDAQ system. Seven additional analog inputs are used to log the control surface deflections by recording the value output by the servo potentiometers. The pilot commands are also recorded by measuring the pulse width modulation (PWM) signals generated by receiver. The motor voltage, current, RPM, and power setting are recorded by FDAQ through an interfaces with the ESC. Given the included sensors, the system is able to simultaneously log and transmit: 3D linear and angular accelerations, velocities, and position along with GPS location; pitot-static probe airspeed; 3D magnetic field strength and heading; control surface inputs; control surface deflections; and motor voltage, current, RPM, and power.

American Institute of Aeronautics and Astronautics

C. Baseline Aircraft Specifications

The completed flight-ready aircraft physical specifications are given in Table 1, and its airframe component specifications are given in Table 2. The performance specifications of the GA-USTAR aircraft instrumentation are given in Table 3 and the component specifications are given in Table 4.

Table 1. Baseline GA-USTAR unmanned aircraft physical specifications.

Geometric Properties	
Overall Length	64.0 in (1630 mm)
Wingspan	81.0 in (2060 mm)
Wing Area	898 in^2 (57.9 dm^2)
Wing Aspect Ratio	7.47
Inertial Properties	
Weight	
Empty (w/o Batteries)	12.08 lb (5.48 kg)
8S 6.6 Ahr LiPo Main Battery	2.74 lb (1.25 kg)
RC and Avionics Batteries	0.49 lb (0.22 kg)
Gross Weight	15.31 lb (6.94 kg)
Wing Loading	39.3 oz/ft^2 (120 gr/dm^2)

Table 2. Baseline GA-USTAR unmanned aircraft airframe component specifications.

Airframe	
Model	Top Flite 1/5-scale Cessna 182
Construction	Built-up balsa and plywood structure, aluminum landing gear, fiberglass cowl, fiberglass wheel pants, and styrene canopy.
Flight Controls	
Control Surfaces	(2) Ailerons, (2) elevator, rudder, (2) flap, and throttle
Transmitter	Futaba T14MZ
Receiver	Futaba R6008HS
Servos	(7) Futaba S3010
Power Distribution	SmartFly PowerSystem Sport Plus
Receiver Battery	(2) Thunder Power ProLite RX 25c 2S 7.4V 1350 mAh
Propulsion	
Motor	Hacker A50-14L Outrunner
ESC	Castle Creations
Propeller	APC Thin Electric 16x8
Motor Flight Pack	(4) Thunder Power ProLite 25c 8S 6600 mAh
Motor Power Switch	Emcotec SPS 60/120

American Institute of Aeronautics and Astronautics

Table 3. Performance specifications of the GA-USTAR aircraft instrumentation.

Sensors	
Inertial sensors	3-axis, ±5 g accelerometer 3-axis, ±300 deg/s gyroscope
Magnetometers	3-axis ±750 mG and 3-axis ±11 G
Altimeter (barometric)	1 ft resolution
Airspeed (pitot probe)	5–120 mph, 0.1 mph resolution
GPS position	Up to 400 Hz (IMU assisted)
Tachometer	Motor ESC based
PWM inputs	Up to 22
Analog inputs	Up to 32x 0-5V 12 bit
Data Handling	
Rate	400 Hz
Storage	32 GB
Local output	Serial or Ethernet
RF link	900 MHz

Table 4. Component specifications of the GA-USTAR aircraft instrumentation.

Data acquisition system	Al Volo FDAQ 400 Hz system
Inertial and Flow Sensors	
Inertial measurement unit	XSens MTi-G-700 AHRS with GPS
Airspeed probe	EagleTree Systems pitot-static probe
Airspeed sensor	All Sensors 20cmH2O-D1-4V-MINI differential pressure sensor
Motor Sensors	Castle Creations Serial Link connected to FDAQ motor sensor input
Power	
Regulator	Built into FDAQ
Battery	Thunder Power ProLite 3S 1350 mAh

American Institute of Aeronautics and Astronautics

III.   Data Reduction

Flight measurements will be captured by the FDAQ using a 9 degree-of-freedom inertial measurement unit with GPS receiver, a pitot-static probe, analog input from hall effect rotary position sensors, pulse width modulation (PWM) signal inputs, and a motor-controller interface. Using these aforementioned sensors and data sources, the FDAQ data acquisition system is able to collect the following data:

- accelerations in body-frame (a_x, a_y, and a_z) and velocities in inertial-frame (V_N, V_E, and V_D), and positions in inertial-frame (x, y, and z in ENU)

- rotation rates in body-frame (p, q, and r) and euler angles (ϕ, θ, and ψ)

- flow conditions including airspeed (V), static pressure(P), and ambient temperature(T)

- control surface deflections for right and left ailerons, right and left elevators, rudder, and right and left flaps

- motor state including rotation rate, voltage, current, and throttle percentage.

However, in order to use the flight data collected for model development, additional calculations are needed. It is desired that velocity be expressed in a body-frame coordinate system (u, v, and w) and with that, flow angles for angle of attack (α) and sideslip (β) be known. Body-frame velocities are found by performing rotations as such

$$
\begin{bmatrix} u \\ v \\ w \end{bmatrix} = R_I^B(\phi, \theta, \psi) \begin{bmatrix} V_N \\ V_E \\ V_D \end{bmatrix}
\tag{1}
$$

where,

$$
R_I^B(\phi, \theta, \psi) = \begin{bmatrix} 1 & 0 & 0 \\ 0 & \cos\phi & \sin\phi \\ 0 & -\sin\phi & \cos\phi \end{bmatrix} \begin{bmatrix} \cos\theta & 0 & -\sin\theta \\ 0 & 1 & 0 \\ \sin\theta & 0 & \cos\theta \end{bmatrix} \begin{bmatrix} \cos\psi & \sin\psi & 0 \\ -\sin\psi & \cos\psi & 0 \\ 0 & 0 & 1 \end{bmatrix}
\tag{2}
$$

Once the body-frame velocities are known, the flow angles can be calculated by

$$
\alpha = \tan^{-1}(w/u)
\tag{3a}
$$

$$
\beta = \sin^{-1}(v/V)
\tag{3b}
$$

It should be noted that a no-wind assumption is made following the conditions observed during flight testing. Otherwise, wind would need to be considered in the above computations.[21]

American Institute of Aeronautics and Astronautics

IV.   Flight Testing and Results

Over a dozen flight tests were performed with the 1/5-scale Cessna 182 baseline aircraft (GA-USTAR Phase 1 Platform). Each of the flight tests performed spanned approximately 20 mins and the flight data collected during these flights was post-processed at the field to verify the data acquired. The data presented includes control surface deflections (R/L ailerons, R/L elevators, rudder, and R/L flaps), position (in NED), velocities (u, v, and w), accelerations (A_x, A_y, and A_z), euler angles (ϕ, θ, and ψ), rotation rates (p, q, and r), and flow angles (α and β). It should be noted that all of the maneuvers presented were performed power-off (zero motor power).

The list of flight test maneuvers performed for the purpose of aerodynamic model validation is listed in Table 5.

Table 5. Flight Test Maneuvers Performed by Baseline GA-USTAR Aircraft

Maneuver	Flight Configuration	Description
Idle Descent	Clean	Trimmed descent using idle power
Phugoid Dynamics	Clean	Trimmed conditions;
		apply elevator deflection to change
		airspeed by 5-10 knots; hands off for 3 full cycles
Roll Response (Rate)	Clean	Roll rate measured through at least
		30 deg of roll. Aileron control
		deflected 1/3 of maximum travel.
Rudder Response	Clean	Use 25 % of maximum rudder deflection
Power-Off Stall	Clean	Stall entry at wings level (1g);
		limited elevator deflection
Power-Off Stall	Clean	Stall entry at wings level (1g):
		full elevator deflection
Power-Off Stall	Half-Flaps	Stall entry at wings level (1g)

American Institute of Aeronautics and Astronautics

A. Idle Descent (Glide)

The idle descent (glide) flight maneuver is performed as a method of ensuring that the parasitic drag contributions of the flight simulator aerodynamic model are correctly characterized. Prior to performing this maneuver, the baseline GA-USTAR aircraft was trimmed to the 50% throttle configuration. Figure 3 shows the trajectory of the aircraft in idle descent flight while a time history of aircraft state is given in Fig. 4. The altitude was observed to decrease approximately 30 m over 10 s [Fig. 4(c)]. During that period, all control surfaces were held constant [Figs. 4(a,b)]. The Euler angles of the aircraft were observed to be relatively constant with a constant bank angle observed [Fig. 4(d)]. As expected, the roll and pitch rotation rates [Fig. 4(f)], although noisy, averaged to approximately 0 deg/s while the yaw rate was approximately 2 deg/s resulting from the slight bank angle. The airspeed was observed to be approximately at 20 m/s (45 mph)[Fig. 4(g)].
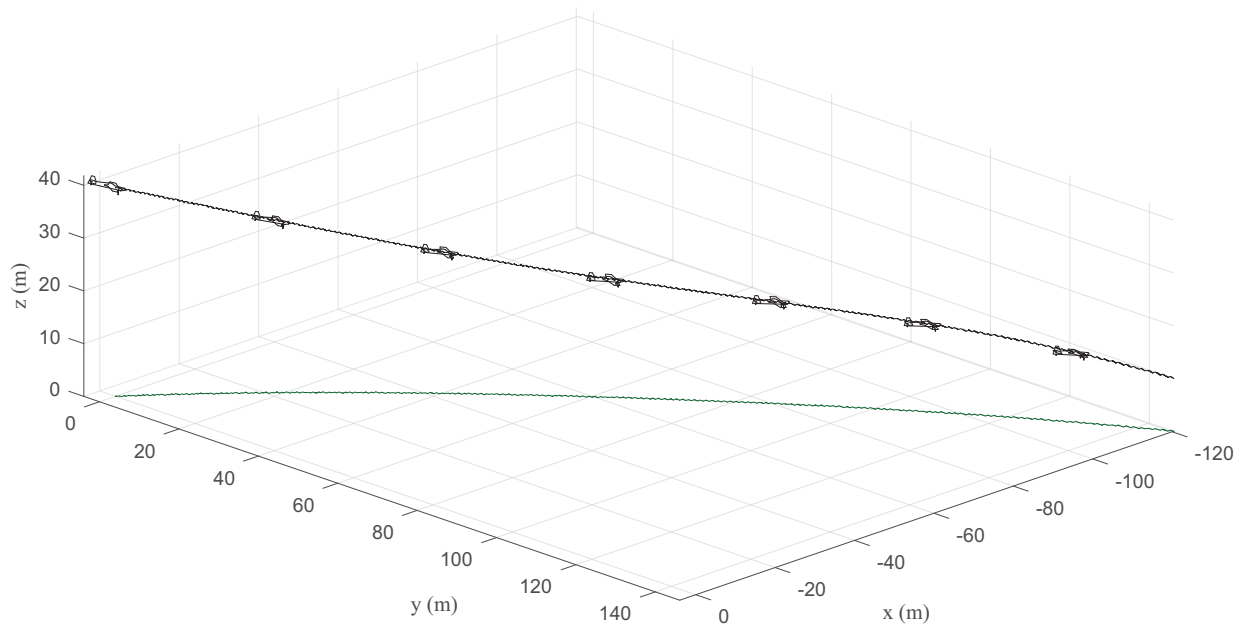
Figure 3. Trajectory plot of idle descent (glide) flight (the aircraft is drawn four times larger than the actual size and once every 1.5 s).

American Institute of Aeronautics and Astronautics
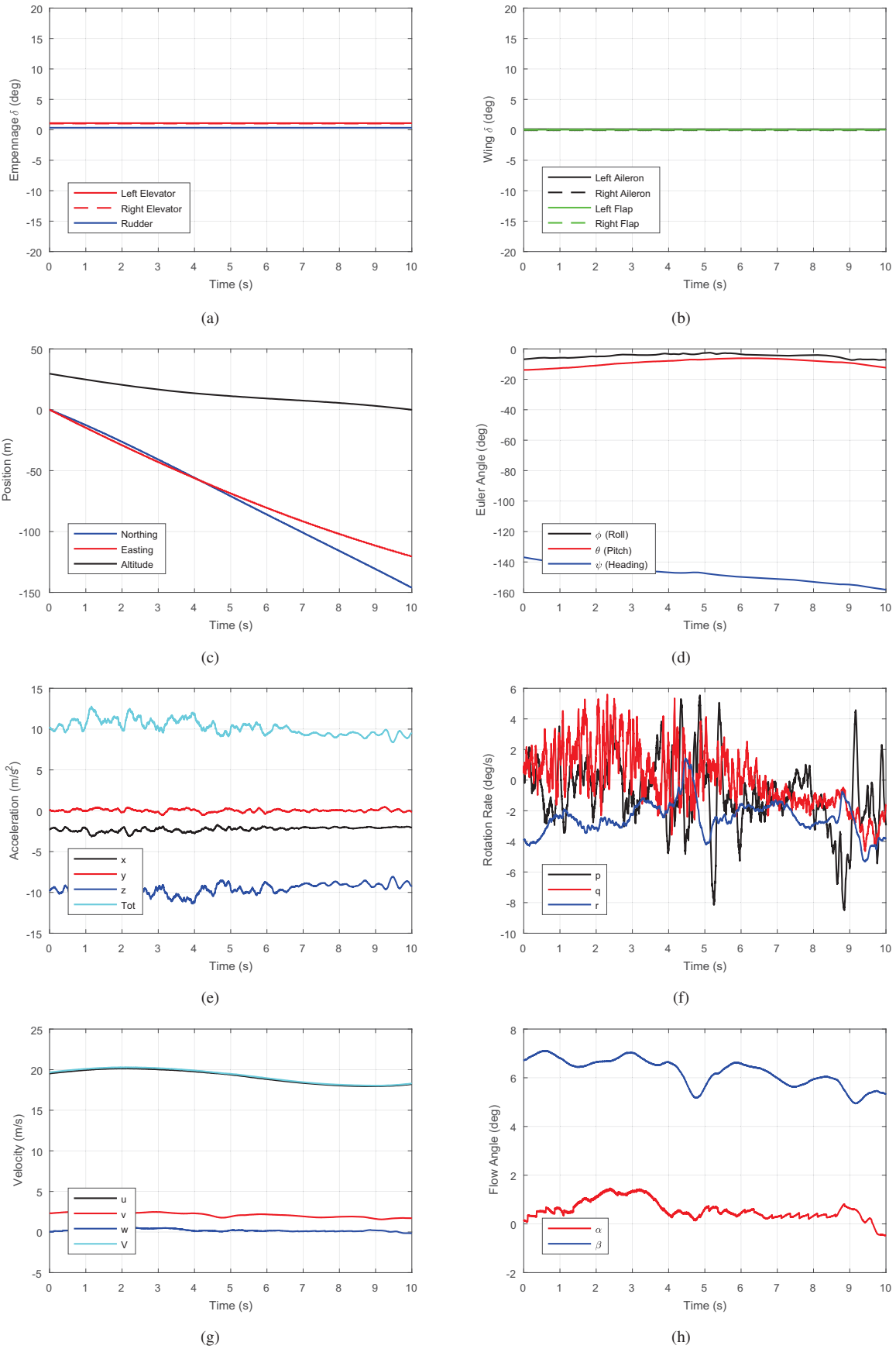
Figure 4. A time history of the GA-USTAR aircraft state during idle descent (glide) flight.

American Institute of Aeronautics and Astronautics

B. Phugoid Dynamics

The phugoid dynamics of the baseline GA-USTAR model was tested to demonstrate the dynamic longitudinal stability of the aircraft. Figures 5 and 6 show the trajectory and time history of the aircraft performing a phugoid. As the time history shows, the maneuver was preceded by trimmed gliding flight at 20 m/s (45 mph) for approximately 6 s. The elevators were then deflected to 11 deg for approximately 1 s start the phugoid oscillation. No other control actuation was performed during the rest of the time history.

During the elevator actuation, an acceleration of 10 m/s^2 and pitch rate of up to 50 deg/s is observed [Fig. 6(f)]. The rotation causes the pitch to increase to approximately 25 deg and the angle of attack to increase to 10 deg. The velocity drops by approximately 5 m/s. The pitch-rate and associated airspeed and pitch changes seem to exhibit unsteady aerodynamic effects (i.e., large change in pitch with drop in airspeed to less than stall speed). There is a slight roll angle at the beginning of the maneuver, which causes a side-slip. Both the roll angle and side-slip seem to increase as a result of elevator deflection and then both return to their initial values after 5 s.

After the elevator deflection actuation ends, the aircraft begins to pitch down with a hump in rotation, as can be seen in Fig. 6 (f). The aircraft then oscillates an additional pitch cycle; the angle of attack exhibits approximately the same behavior. During the pitching oscillation, the velocity and corresponding altitude oscillates as well.
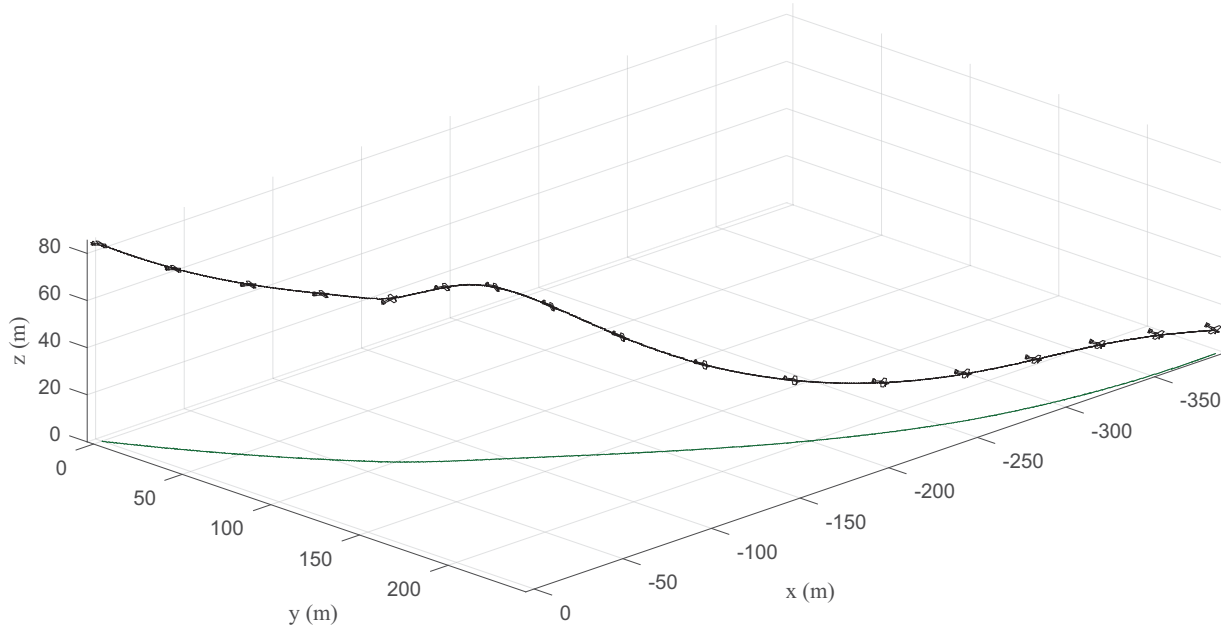

Figure 5. Trajectory plot of a phugoid (the aircraft is drawn four times larger than the actual size and once every 1.5 s).
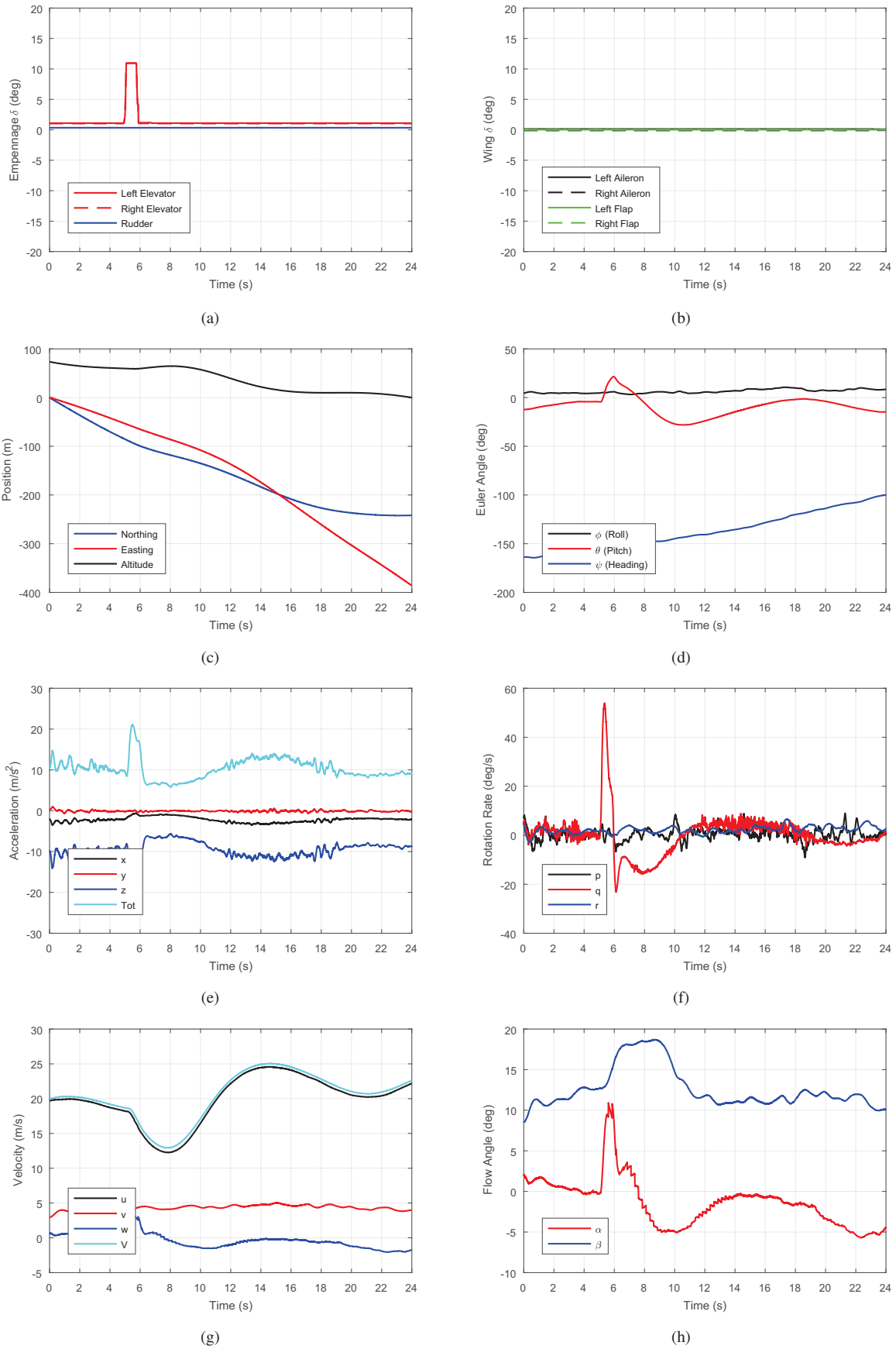
American Institute of Aeronautics and Astronautics

(a)

(b)

(c)

(d)

(e)

(f)

(g)

(h)

Figure 6. A time history of the GA-USTAR aircraft state during a phugoid.

American Institute of Aeronautics and Astronautics

C.   Roll Response

Roll response maneuvers were performed to characterize the dynamics of the baseline GA-UTAR aircraft under a 30 deg rapid roll angle change. The effects captured here that need to be matched in the flight simulator include apparent mass effects and induced angle of attack variations along the wing.

Figure 7 shows the trajectory of the aircraft in roll response flight. The time history of aircraft state is given in Fig. 8. It can be seen in Fig. 8 (b), that the ailerons are instantaneously actuated to 14 deg right and left, with about 2 s between each actuation. Figure 8 (f) shows that the actuation causes roll rates of 100 to 120 deg/s. There are some effect to pitch, which is rather minimal, while there are significant effects to aircraft heading; these effects can be seen in Fig. 8 (d) and (f). With the aileron actuation, there are significant changes in both angle of attack and side-slip. During the manuevers, aircraft total velocity does not seem to be significantly affected although a visible shift between forward to sidewards velocity is observed.
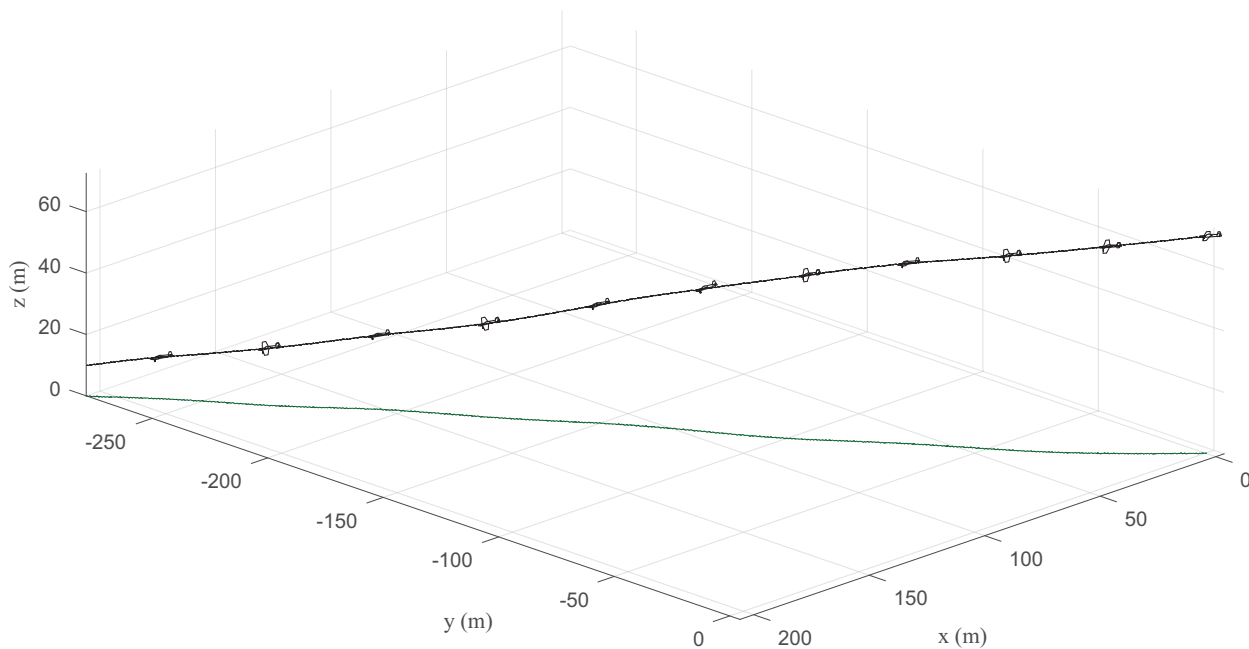
Figure 7.   Trajectory plot of aileron response flight (the aircraft is drawn four times larger than the actual size and once every 1.5 s).
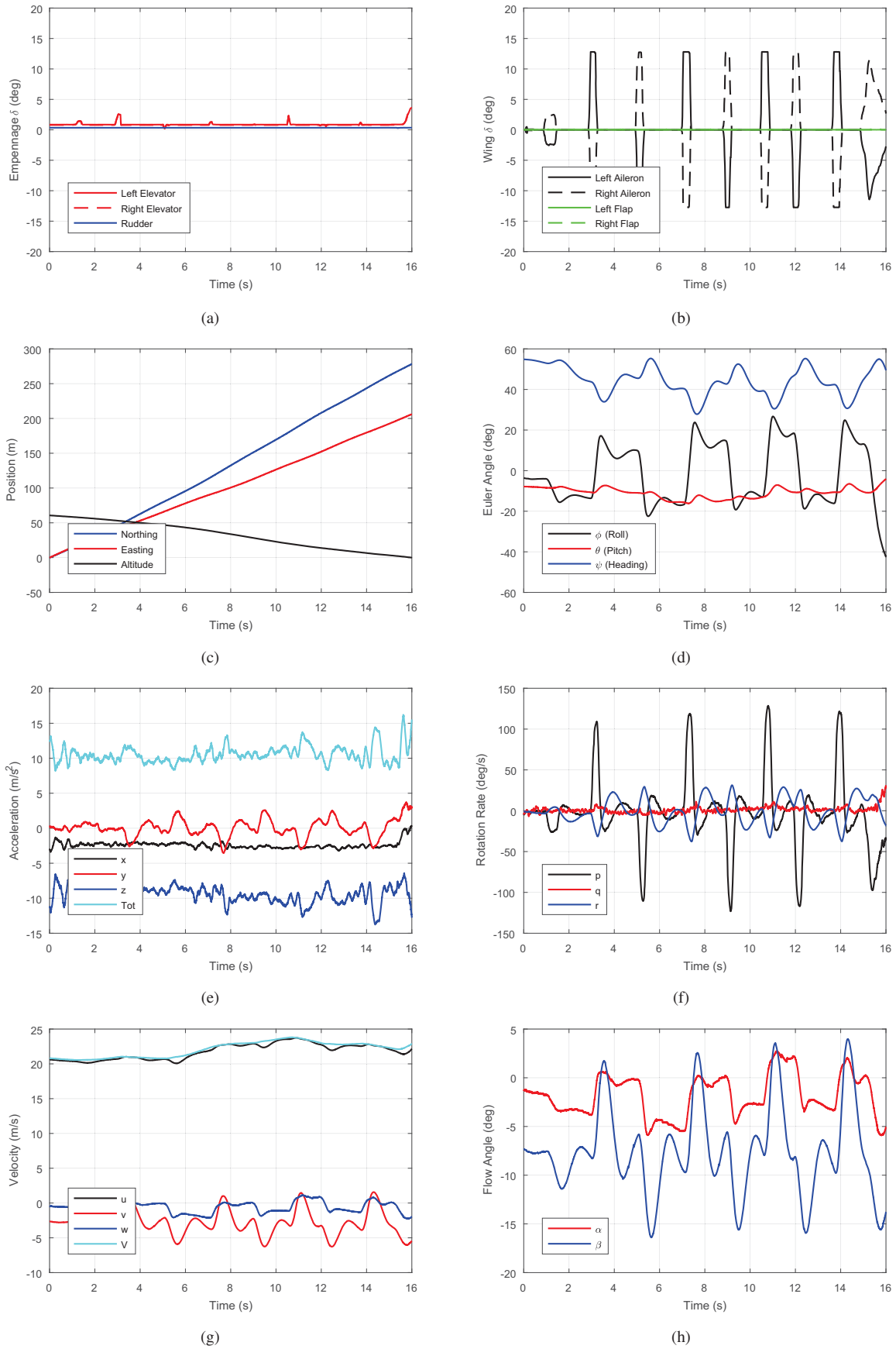
American Institute of Aeronautics and Astronautics

(a)

(b)

(c)

(d)

(e)

(f)

(g)

(h)

Figure 8. A time history of the GA-USTAR aircraft state during aileron response flight.

D.   Rudder Response Flight

Similar to the roll response maneuver, rudder response was conducted by applying a rudder step input and observing the induced dynamics due to this step input. Figure 9 shows the trajectory of the aircraft in rudder response flight. The time history of the aircraft state is given in Fig. 10. It can be seen in Fig. 10 (b), that the rudder is instantaneously actuated to 14 deg right and left, with approximately 2 s between each actuation. Figure 8 (f) shows that the actuation causes roll and yaw rates of between 40 and 100 deg/s depending on the length of actuation; there is also a discernible effect to pitch also visible. The rudder actuation also significantly affects angle of attack and side-slip as can be seen in Fig. 10 (h).
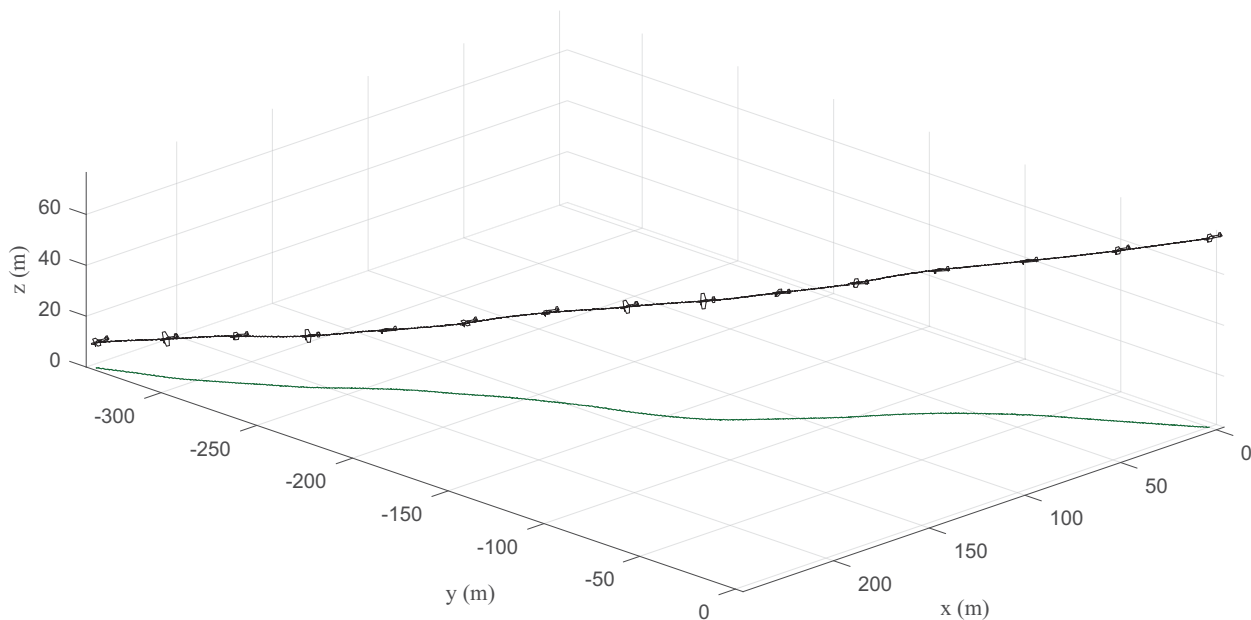
Figure 9. Trajectory plot of rudder response flight (the aircraft is drawn four times larger than the actual size and once every 1.5 s).
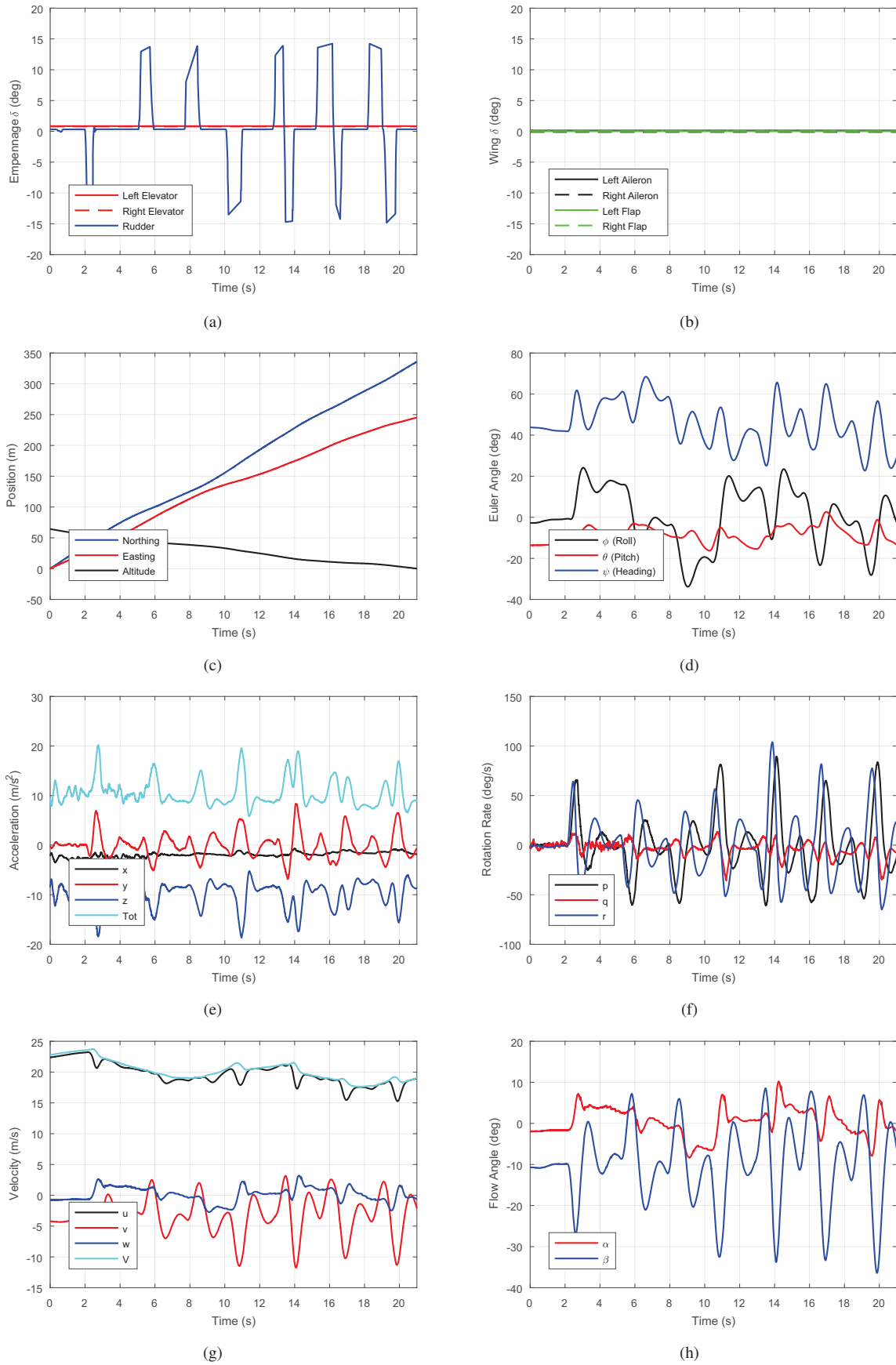
American Institute of Aeronautics and Astronautics

Figure 10. A time history of the GA-USTAR aircraft state during rudder response flight.

American Institute of Aeronautics and Astronautics

E.   Stall with Low Rate Elevator and without Flaps

A stall with low rate (11 deg) elevator and without flaps was performed to capture characteristics related to the baseline GA-USTAR in slow flight or flight close to stall. Figures 11 and 12 show the trajectory and time history of the stall. Over the first 5 s, the aircraft transitioned from a glide at approximately 21 m/s, to a stall at 16 m/s, with altitude being maintained. The elevator was gradually increased to full low rate deflection of 11 deg at which point the stall occurred. The aircraft was at an angle of attack of approximately 12 deg. Afterward for approximately the next 10 s, the full low rate deflection of 11 deg was maintained, during which the aircraft remained in what is described a mush stall. During the mush, the aircraft oscillated in angle of attack between the 12 deg, which began the stall, to 10 deg, and then back to 12 deg.

At the beginning of the maneuver, there was an approximately 10 deg roll angle and with that sideslip. This roll angle and sideslip increased as the aircraft was stalled. It is interesting to note that the sideslip angle had an oscillation that looked to be aligned with the oscillation of angle of attack during the mush stall.

The stall ended with the elevator being actuated back to 0 deflection, allowing the aircraft to recover. The recovery began with a velocity of 14 m/s, with the velocity rapidly increasing. The aircraft was observed to rapidly pitch down at a rate of 25 deg/s for a brief moment followed by a slower pitch rate change that eventually transitions into the aircraft pitching up. The recovery looks to be the beginnings of a phugoid.
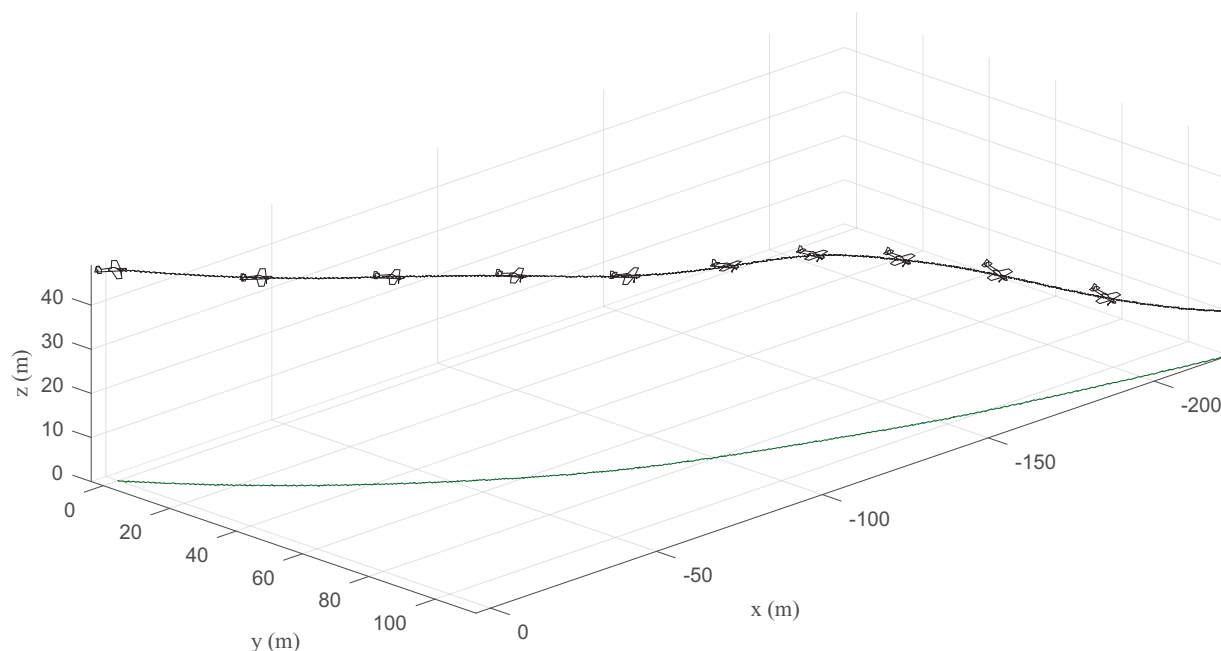

Figure 11.   Trajectory plot of a stall with low rate elevator and without flaps (the aircraft is drawn four times larger than the actual size and once every 1.5 s).
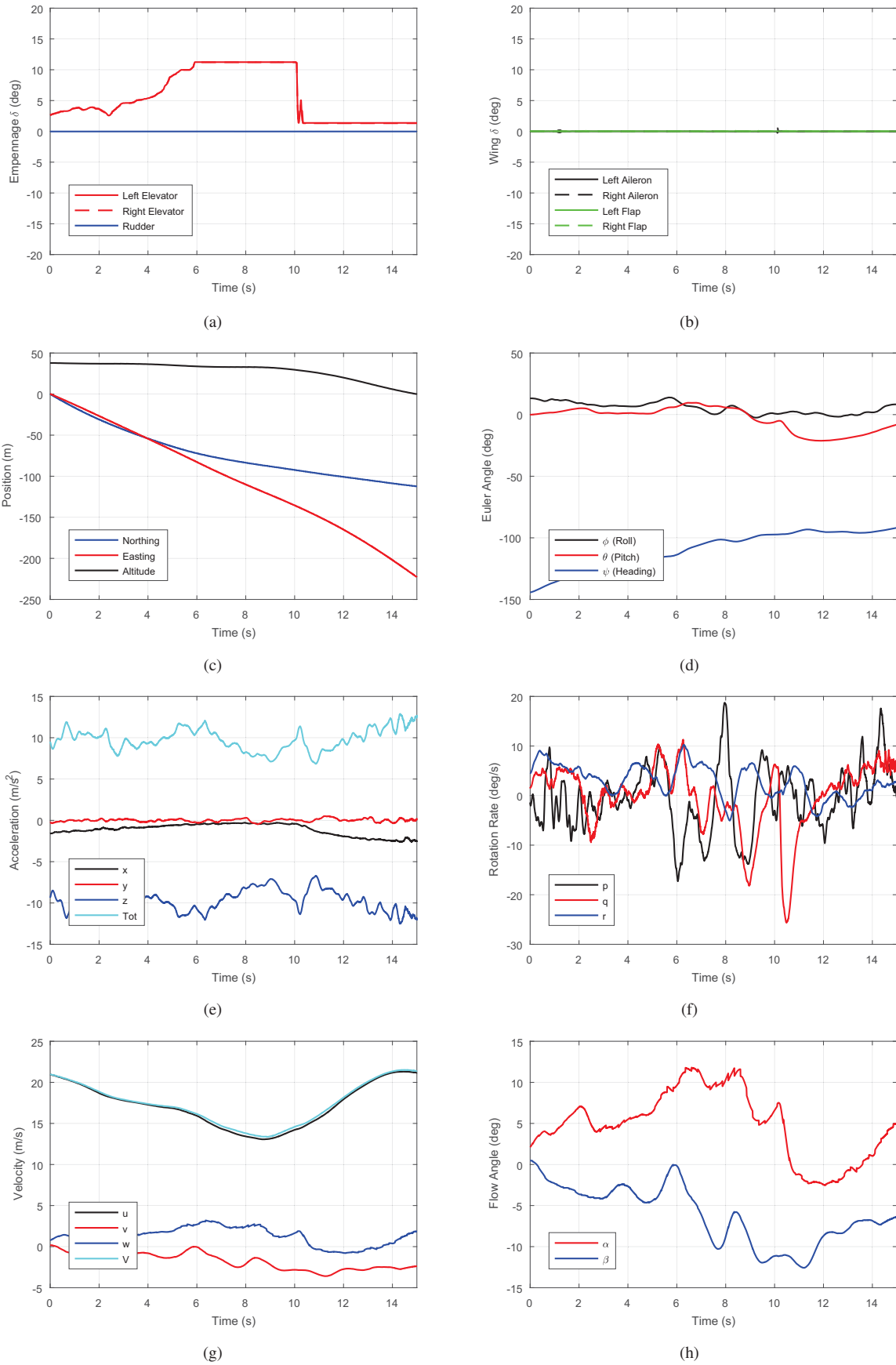
American Institute of Aeronautics and Astronautics

(a)

(b)

(c)

(d)

(e)

(f)

(g)

(h)

Figure 12. A time history of the GA-USTAR aircraft state during a stall with low rate elevator and without flaps.

American Institute of Aeronautics and Astronautics

F. Stall with High Rate Elevator and without Flaps

A stall with high rate (15 deg) elevator and without flaps was performed to capture the aerodynamic characteristics of the GA-USTAR in power-off stall in the clean (no flaps) condition. The stall entry and upset conditions are captured in this maneuver. Figures 13 and 14 show the trajectory and time history of the stall. Over the first 7 s, the aircraft transitioned from a glide at approximately 15 m/s, to a stall at 9 m/s, with altitude being maintained. The elevator was gradually increased to full high rate deflection of 15 deg at which point the stall occurred. The aircraft stalled at an angle of attack of approximately 16 deg. Some aileron deflection was used to keep the wing level, i.e., keep the aircraft at 0 roll angle. However, it is important to note that there was no aileron deflection for more than the last two seconds before the stall occurred. Once the aircraft stalled, a rightward spin was initiated. The elevator was then returned to 0 deg of deflection to end the spin. A recovery, not shown in the time history, was performed.
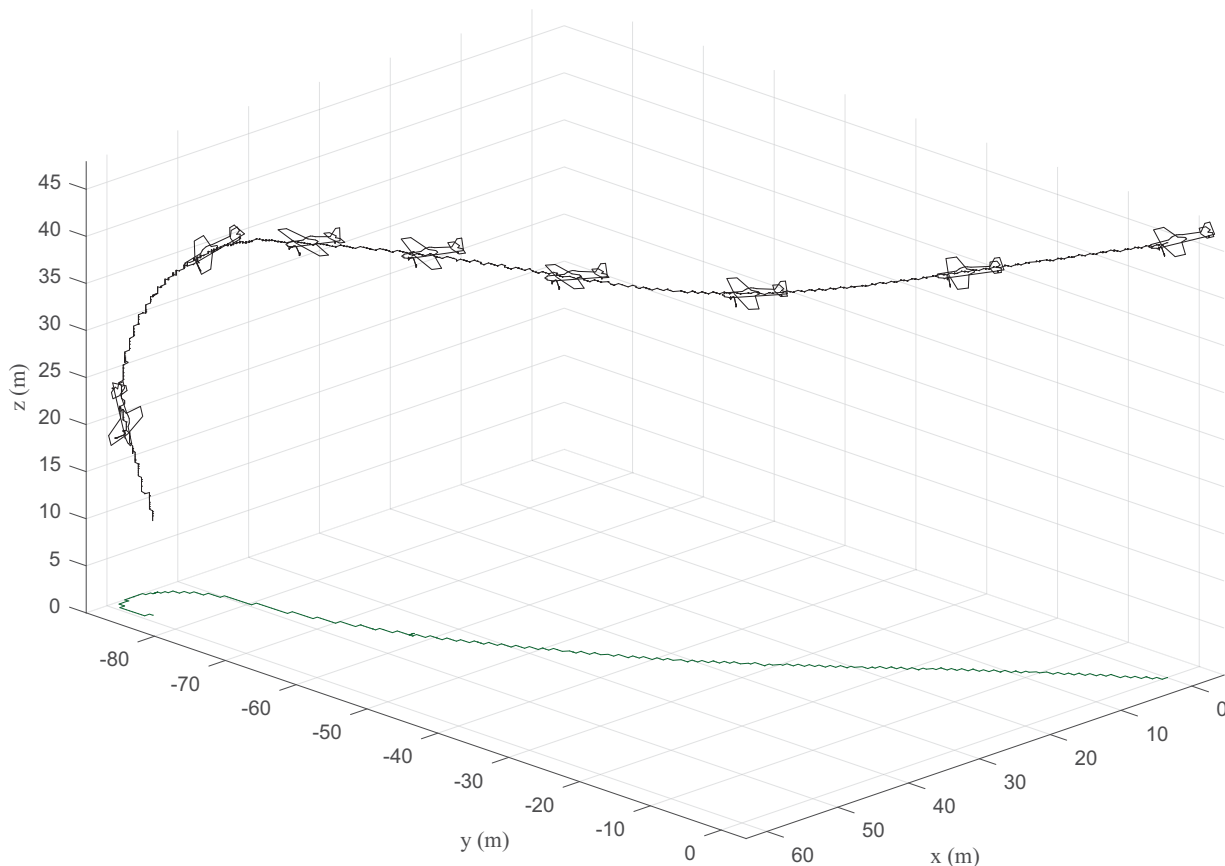

Figure 13. Trajectory plot of a stall with high rate elevator and without flaps (the aircraft is drawn four times larger than the actual size and once every 1.5 s).
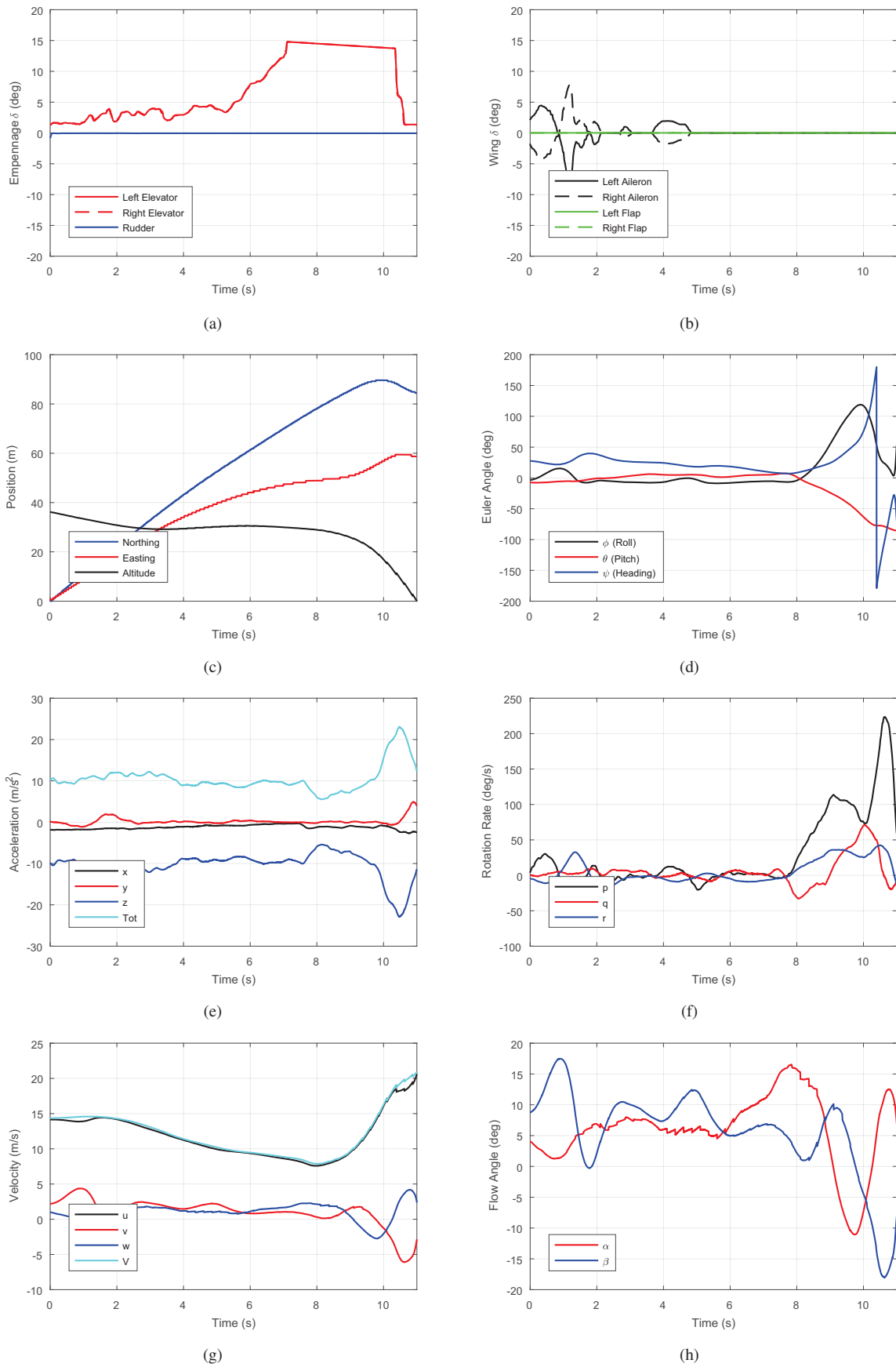
American Institute of Aeronautics and Astronautics

(a)

(b)

(c)

(d)

(e)

(f)

(g)

(h)

Figure 14. A time history of the GA-USTAR aircraft state during a stall with high rate elevator and without flaps.

American Institute of Aeronautics and Astronautics

G. Stall with High Rate Elevator and Half Flaps

A stall with high rate (15 deg) elevator and half flaps (18 deg) was performed to capture the dynamics of the baseline GA-USTAR aircraft in power-off stall in the landing/approach configuration.

Figures 15 and 16 show the trajectory and time history of the stall. Over the first 7 s, the aircraft transitioned from a glide at approximately 17 m/s, to a stall at 14 m/s, with altitude being maintained. The elevator was gradually increased to full high rate deflection of 15 deg at which point the stall occurred. The aircraft stalled at an angle of attack of approximately 16 deg. Some aileron deflection was used to keep the wing level, i.e. keep the aircraft at 0 roll angle. Again, it is important to note that there was no aileron deflection for more than the last four seconds prior to the stall occurring. Once the aircraft stalled, a leftward spin was initiated. The elevator was then briefly returned to 0 deg of deflection to end the spin followed by a recovery, the beginnings of which are visible in the time history.
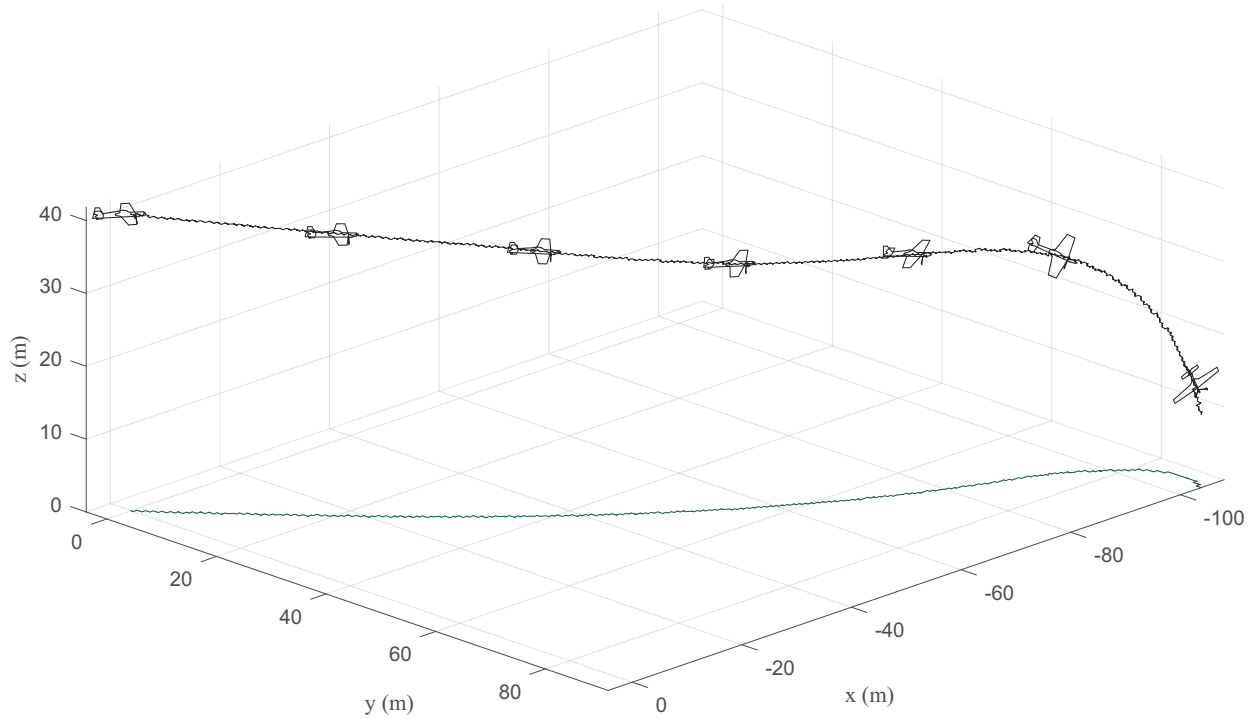

Figure 15. Trajectory plot of a stall with high rate elevator and half flaps (the aircraft is drawn four times larger than the actual size and once every 1.5 s).
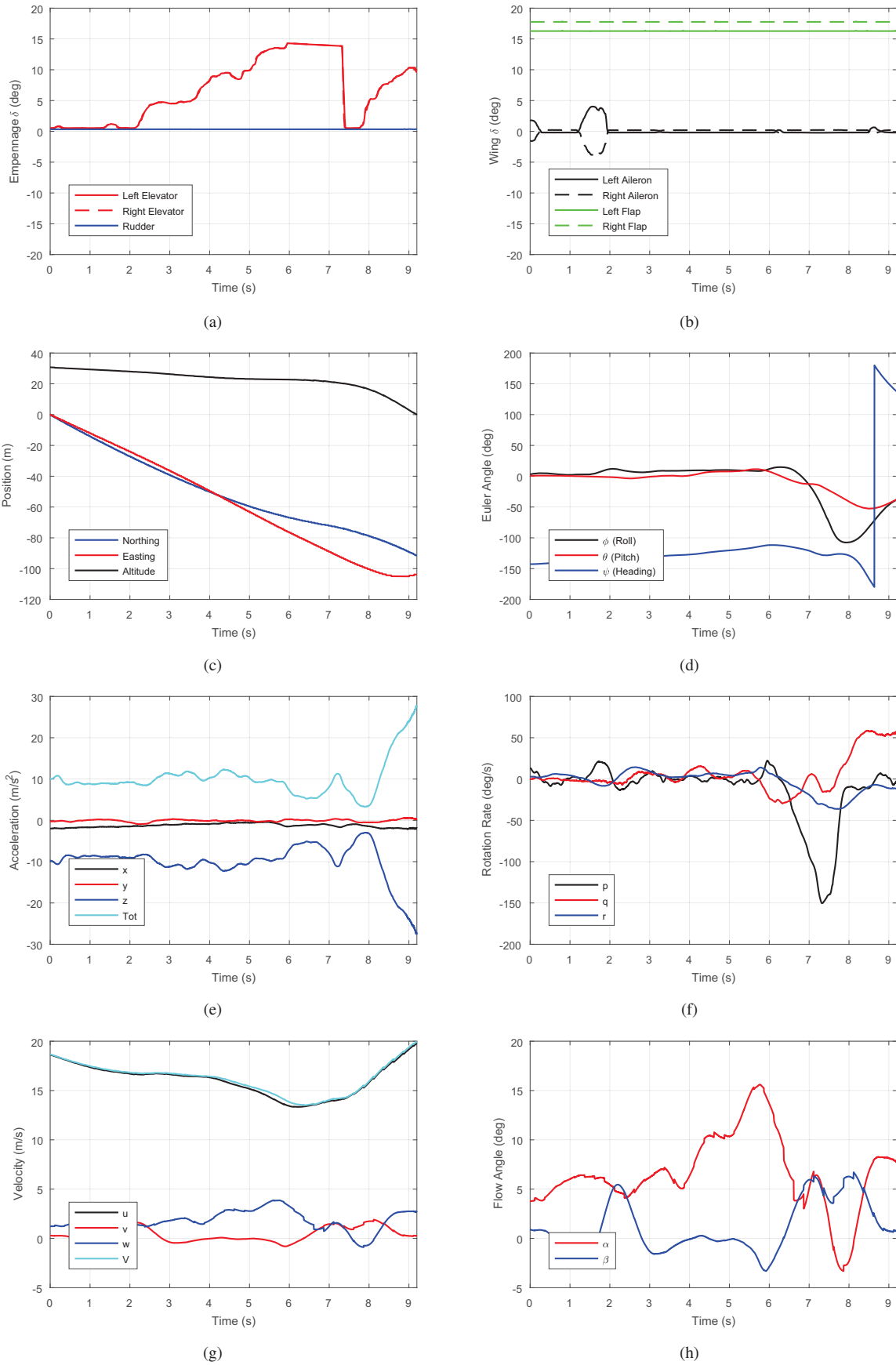
American Institute of Aeronautics and Astronautics

(a)

(b)

(c)

(d)

(e)

(f)

(g)

(h)

Figure 16. A time history of the GA-USTAR aircraft state during a stall with high rate elevator and half flaps.

American Institute of Aeronautics and Astronautics

V.   Conclusions and Future Work

This paper described the development and flight testing of the baseline aircraft for the GA-USTAR project, which aims to develop a dynamically- scaled, Reynolds number corrected, scale GA aircraft to provide validation data sets for the stall/upset aerodynamic model development. As such, a 1/5- scale Cessna 182 was first built as a radio control model with modifications being made to support future GA-USTAR project activities. The aircraft was instrumented with a high-fidelity data acquisition system, which was then used to collect baseline flight characteristics. An extensive set of flight testing results were presented including idle decent (gliding), elevator-induced phugoid, aileron roll rate response, rudder response, stall with low rate elevator and without flaps, stall with high rate elevator and without flaps and finally stall with high rate elevator and half flaps.

The work presented in this paper is an important stepping stone in the GA- USTAR project. The flight data generated from the baseline GA-USTAR aircraft will soon be used in validating aerodynamic models developed and as first step toward making a high-fidelity stall/upset aerodynamic model. Additionally, moment of inertia testing will soon be performed to parameterize the current baseline aircraft. This testing shall facilitate Phase 2 of this project, where the aircraft will be dynamically scale through the a redesign of the wings and strategic placement of weights. This will be followed by Phase 3 with a new Reynolds number corrected wing being developed.

Acknowledgments

References

[1]Ananda, G. K., Vahora, M., Dantsker, O. D., and Selig, M. S., "Design Methodology and Flight-Testing Protocols for a Dynamically-Scaled General Aviation Aircraft," AIAA Paper 2017-4077, AIAA Applied Aerodynamics Conference, Denver, Colorado, Jun 2017.

[2]Dickes, E. G., Ralston, J. N., and Lawson, K. P., "Application of Large-Angle Data for Flight Simulation," AIAA Paper 2000-4584, Denver, Colorado, August 2000.

[3]Donaldson, S., Priest, J., Cunningham, K., and Foster, J. V., "Upset Simulation and Training Initiatives for U.S. Navy Commercial Derived Aircraft," AIAA Paper 2012-4570, Minneapolis, Minnesota, August 2012.

[4]National Transportation Safety Board, "Review of U.S. Civil Aviation Accidents: Review of Aircraft Accident Data 2010," NTSB ARA-12/01, Washington D.C., 2010.

[5]National Transportation Safety Board, "NTSB 2015 Most Wanted Transportation Safety Improvements: Prevent Loss of Control in Flight in General Aviation," NTSB Brochure, Washington D.C., 2015.

[6]National Transportation Safety Board, "NTSB 2016 Most Wanted Transportation Safety Improvements: Prevent Loss of Control in Flight in General Aviation," NTSB Brochure, Washington D.C., 2016.

[7]National Transportation Safety Board, "NTSB 2017 Most Wanted Transportation Safety Improvements: Prevent Loss of Control in Flight in General Aviation," NTSB Brochure, Washington D.C., 2017.

[8]Jordan, T. L., Langford, W. M., Belcastro, C. M., Foster, J. M., Shah, G. H., Howland, G., and Kidd, R., "Development of a Dynamically Scaled Generic Transport Model Testbed for Flight Research Experiments," Tech. rep., AUVSI, Arlington, VA, 2004.

[9]Jordan, T. L., Langford, W. M., and Hill, J. S., "Airborne Subscale Transport Aircraft Research Testbed – Aircraft Model Development," AIAA Paper 2005-6432, San Francisco, CA, August 2005.

[10]Bailey, R. M., Hostetler, R. W., Barnes, K. N., and Belcastro, C. M., "Experimental Validation: Subscale Aircraft Ground Facilities and Integrated Test Capability," AIAA Paper 2005-6433, San Francisco, CA, August 2005.

[11]Cunningham, K., Foster, J. V., Morelli, E. A., and Murch, A. M., "Practical Application of a Subscale Transport Aircraft for Flight Research in Control Upset and Failure Conditions," AIAA Paper 2008-6200, Honolulu, Hawaii, August 2008.

[12]Hobbico, Inc., "Top Flite Cessna 182 Skylane 60 ARF," http://www.top-flite.com/airplanes/topa0906.html, Accessed Oct. 2016.

[13]Al Volo LLC, "Al Volo: Flight Data Acquisition Systems," http://www.alvolo.us, Accessed Jun. 2017.

[14]Xsens Technologies B.V., "XSens, MTi-G-700," https://www.xsens.com/products/mti-g-700/, Accessed Jan. 2016.

[15]Federal Aviation Administration, "14 CFR Part 60 : Flight Simulation Training Device Qualification Standards for Extended Envelope and Adverse Weather Event Training Tasks; Final Rule," Federal Register Vol. 81, No. 16, Department of Transportation, 2016.

[16]Ananda, G. K. and Selig, M. S., "Stall/Post-Stall Modeling of the Longitudinal Characteristics of a General Aviation Aircraft," AIAA Paper 2016-3541, AIAA Aviation 2016, Atmospheric Flight Mechanics Conference, Washington, D.C., June 2016.

American Institute of Aeronautics and Astronautics

[17]Dantsker, O. D., Johnson, M. J., Selig, M. S., and Bretl, T. W., "Development of the UIUC Aero Testbed: A Large-Scale Unmanned Electric Aerobatic Aircraft for Aerodynamics Research," AIAA Paper 2013-2807, AIAA Applied Aerodynamics Conference, San Diego, California, Jun. 2013.

[18]Ragheb, A. M., Dantsker, O. D., and Selig, M. S., "Stall/Spin Flight Testing with a Subscale Aerobatic Aircraft," AIAA Paper 2013-2806, AIAA Applied Aerodynamics Conference, San Diego, CA, Jun. 2013.

[19]Dantsker, O. D. and Selig, M. S., "High Angle of Attack Flight of a Subscale Aerobatic Aircraft," AIAA Paper 2015-2568, AIAA Applied Aerodynamics Conference, Dallas, Texas, Jun. 2015.

[20]Quest Engineering & Development, Inc., "Smart-Fly," http://www.smart-fly.com/, Accessed Nov. 2012.

[21]Beard, R. W. and McLain, T. W., *Small Unmanned Aircraft: Theory and Practice*, Princeton University Press, Princeton, NJ, 2012.